Experimental Evaluation of Layout Designs for 3×3 MIMO-Enabled Radio-over-Fiber Distributed Antenna Systems

George S.D. Gordon, *Student Member, IEEE,* Michael J. Crisp, *Member, IEEE,*
Richard V. Penty, *Senior Member, IEEE,* and Ian H. White, *Fellow, IEEE*

***Abstract*—This paper demonstrates experimentally that for two representative indoor distributed antenna system (DAS) scenarios, existing radio-over-fiber (RoF) DAS installations can enhance the capacity advantages of broadband 3×3 multiple-input multiple-output (MIMO) radio services without the requirement for additional fibers or multiplexing schemes. This is true for both the single user and multiple user cases with single and multiple base stations.**

First, a theoretical example is used to illustrate that there is negligible SNR improvement when using a MIMO DAS with all N spatial streams replicated at N remote antenna units compared with a MIMO DAS with only one of the N streams at each remote antenna unit for $N \leq 4$.It is then confirmed experimentally that a 3×3 MIMO DAS offers improved capacity and throughput compared with a 3×3 MIMO collocated antenna system (CAS) for the single-user case in two typical indoor DAS scenarios – one with significant line-of-sight (LOS) propagation and the other entirely non-line-of-sight (NLOS). The improvement in capacity is 3.2% and 4.1% respectively.

Next, experimental channel measurements confirm there is negligible capacity increase of the 3×3 configuration with 3 spatial streams per antenna unit over the 3×3 with a single spatial stream per antenna unit. The former layout is observed to provide an increase of $\sim$1% in the median channel capacity in both the single and multiple user scenarios. With 20 users and 3 base stations a MIMO DAS using the latter layout offers median aggregate capacities of 259 bit/s/Hz and 233 bit/s/Hz for the LOS and NLOS scenarios respectively.

It is concluded that DAS installations can further enhance the capacity offered to multiple users by multiple 3×3 MIMO-enabled base stations. Further, designing future DAS systems to support broadband 3×3 MIMO may not require significant upgrades to existing installations for small numbers of spatial streams.

***Index Terms*—MIMO systems, distributed antenna systems (DAS), radio-over-fiber (RoF).**

I. Introduction

TODAY there are over 5.9 billion mobile subscriptions worldwide and as a result mobile data usage is predicted to increase 18 fold from 2011 to 2016 [1], [2]. Networks are struggling to meet this demand and it is forecast that by 2014 there will be 97% shortfall in capacity [3]. This is particular important for indoor environments where 80-90% of mobile data traffic originates [4]. There are two aspects to addressing this problem – improving coverage, so that wireless service is available everywhere, and adding capacity, so that networks can offer very high data rates to multiple users.

Distributed antenna systems (DAS) are a widespread infrastructure technology capable of providing significant coverage improvement in indoor wireless environments [5]. In contrast to conventional *collocated antenna systems (CAS)*, DASs enable the antennas of wireless base stations to be located remotely from the transceiver hardware and to be duplicated within an environment, thus improving coverage. These remotely located antennas are driven by *remote antenna units* (RAUs). *Radio-over-fiber* (RoF) technology is often used to feed RAUs as it supports long distance transmission of broadband wireless signals [6]. The broadband nature of RoF enables multiple base stations providing different services at different frequencies to operate over a single DAS, termed *multiservice* operation. DAS is a popular coverage improvement solution with over 89,000 installations worldwide [7].

Multiple-input multiple-output (MIMO) is an emerging technology that offers increased capacity for wireless systems. In MIMO systems independent streams of data, called *spatial streams*, are sent from different elements of an M element array of transmit antennas to an N element array of receive antennas (termed an $M \times N$ MIMO system). This allows *spatial multiplexing* so that multiple data streams can be transmitted simultaneously without using extra bandwidth or transmit power, hence greatly increasing the spectral efficiency and available data rate [8]. MIMO is presently being adopted in both wireless LAN (IEEE 802.11n) and mobile (LTE/4G) standards, which allow up for to 4×4 MIMO though only 2×2 and 3×3 systems are commercially available at the time of writing. Standards for future 8×8 MIMO are currently under development, for example IEEE 802.11ac [9].

It remains an important technical challenge to combine the capacity benefits of MIMO with the coverage benefits of DAS. In a generalized MIMO-enabled DAS, it is possible to replicate the M transmitted spatial streams at K remote antenna units (RAUs). This can be done in a number of different ways, two examples of which are shown in figure 1. The key difference is the degree to which spatial streams of each service are replicated at separate RAUs. This can be quantified by introducing a term the *replication factor*, R, defined as:

Manuscript received December 3, 2012; revised May 4, 2013, and July 21, 2013.

The authors are with the Centre for Photonic Systems, Engineering Department, University of Cambridge, CB3 0FA, Cambridge, U.K. (e-mail: gsdg2@cam.ac.uk).

$$R = A = \frac{T}{K} \quad (1)$$

where A is the number of antennas per RAU, T is the total number of antennas in the DAS and K is the number of RAUs.

Previous work has examined two approaches to designing MIMO DASs. The first is to send all MIMO spatial streams to each RAU i.e. an $M \times N$ MIMO DAS with replication factor of $R = M$ such as that of figure 1a. This approach has been shown to provide improved performance over MIMO CAS [10], and a number of multiplexing schemes to provide this functionality over a single fiber have been proposed [11]–[13]. The second approach is to have separate MIMO spatial streams sent to different RAUs, i.e. an $M \times N$ MIMO DAS with replication factor of $R = 1$ such as that of figure 1b. This, too, has been shown to offer improved capacity over co-located MIMO [14], [15]. This approach has the advantage that it does not require additional fibers or multiplexing so can be implemented with minimal upgrades to existing DAS. Hybrids between these two approaches have also been investigated and shown to offer improved capacity for a 2×2 MIMO system [16].

Theoretical work comparing $M \times N$ MIMO DAS with $R = M$ to MIMO DAS with $R = 1$ has found that the former can offer improved capacity [17]. However, these analyses assume ideal composite fading conditions and are for lower receive SNR ($\sim$10dB) than are found in many indoor DAS installations (typically $>$ 20dB). Once the receive SNR is above $\sim$20dB, channel capacity becomes increasingly more sensitive to increases in SNR than to reduced correlation between spatial channels [18]. Though systems can operate well with SNR much lower than 20dB, the maximum channel capacity is directly dependent on SNR so high SNR is desired to provide sufficient capacity to meet user demand.

Simulations of a single service (LTE) DAS supporting 2×2 MIMO in a realistic DAS layout have found that both of the two approaches provide comparable results in terms of capacity [19]. However this has not been verified by experimental measurements nor done for a broadband case. Further, little experimental work has been done on indoor MIMO DAS with 3 or more spatial streams.

Added to this is the increasingly important question of how MIMO systems perform when capacity must be shared amongst multiple users [20]. It has been shown theoretically that in the case of multiple users, DAS provides significant capacity improvements over CAS [21], [22]. However, such work has been largely theoretical and has relied on advanced techniques that are not currently practical to implement.

The aim of this paper, therefore, is to investigate the performance of different designs for 3×3 MIMO DAS from an experimental perspective for two very different propagation scenarios under both single and multiple user access scenarios. Because the experiments are conducted using a commercially available RoF DAS compatible with standard OM1-OM4 multimode optical fiber and the locations of RAUs in the experiments are typical for an indoor DAS installation, the results are immediately applicable to many existing DAS installations.

First, a theoretical justification of metrics used to evaluate the performance of MIMO systems is presented. Next, it is shown theoretically using an illustrative example, that an $N \times N$ MIMO DAS with $R = N$ offers negligible SNR benefit over an $N \times N$ MIMO DAS with $R = 1$ for small N (≤ 4). Because of the strong correlation between SNR and channel capacity in many MIMO scenarios it is reasoned that the two systems should exhibit similar channel capacities.

Following this, it is shown experimentally for the single-user case that a broadband 3×3 MIMO DAS provides improved capacity over CASs. Experiments are conducted in two representative propagation scenarios and it is found that increased SNR is the main factor offering increased capacity, although reduced spatial correlation also has an impact in one of the propagation scenarios. In both cases DAS offers an improvement in both coverage and capacity. This result is then corroborated with throughput measurements using a 3×3 MIMO DAS and an IEEE 802.11n access point.

Then, a 3×3 MIMO DAS with $R = 3$ and a 3×3 MIMO DAS with $R = 1$ are experimentally characterized and compared and it is shown that for the two typical indoor DAS scenarios, the $R = 1$ system offers comparable capacity to the $R = 3$ system for the same total transmit power.

Finally, a multi-user analysis is conducted and the total aggregate capacity of the network is investigated. It is first shown that it is necessary to use multiple base stations to offer significant capacity improvement for multiple users. For the same two indoor environments a number of scenarios are compared – a 3×3 MIMO DAS with $R = 3$ and multiple base stations, a 3×3 MIMO DAS with $R = 1$ and multiple base stations, and the case with 3 separate 3×3 MIMO CAS base stations. It is found that using multiple base-stations over a single DAS provides superior performance to having individual base stations at separate locations. Further, using a 3×3 MIMO DAS with $R = 3$ offers negligible performance advantage over a 3×3 MIMO DAS with $R = 1$.

It is concluded that in realistic DAS installations the existing infrastructure may be capable of supporting the capacity gains of 3×3 MIMO without requiring additional fibers or multiplexing schemes. Further, this holds true for multiple-user systems, provided the DAS can support simultaneous operation of multiple base stations.

II. Theory

A. Single user MIMO

The performance of a MIMO system can be evaluated by calculating the Shannon capacity of the wireless channel it uses. To do this, it is necessary to measure the complex channel transfer coefficients $h_{k,n,m}$ for every possible pair of transmit and receive antennas on the RAU and mobile terminal respectively, as shown in figure 1. For each RAU, k, with M antennas transmitting to N receive antennas on the mobile terminal, these coefficients can be combined into an $N \times M$ matrix $\mathbf{H}_k$:

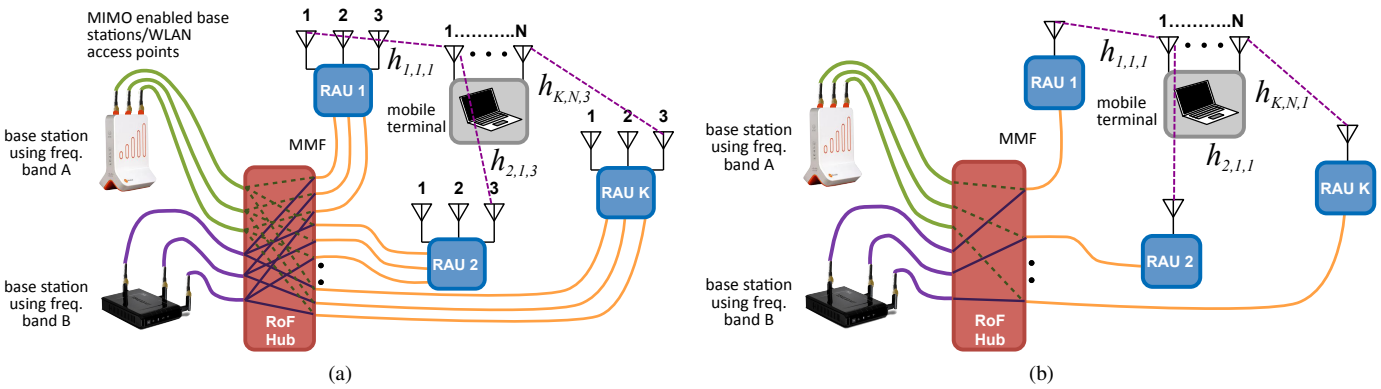

Fig. 1. Example layouts for MIMO DAS with K RAUs supporting two base stations each with 3 spatial channels: (a) replicating all base station antennas at all RAUs – a $3 \times N$ MIMO DAS with a replication factor $R = 3$ and (b) using only one spatial stream at each RAU – a $3 \times N$ MIMO DAS with a replication factor $R = 1$.

$$\mathbf{H}_k = \begin{pmatrix} h_{k,1,1} & h_{k,1,2} & \cdots & h_{k,1,M} \\ h_{k,2,1} & h_{k,2,2} & \cdots & h_{k,2,M} \\ \vdots & \vdots & \ddots & \vdots \\ h_{k,N,1} & h_{k,N,2} & \cdots & h_{k,N,M} \end{pmatrix} \tag{2}$$

The signal received by the mobile terminal from the k^{th} RAU is then given by:

$$\mathbf{y} = \mathbf{H}_k \mathbf{x} + \mathbf{n} \tag{3}$$

where $\mathbf{x}$ is the input signal vector from the base station, $\mathbf{y}$ is the signal vector received by the user and $\mathbf{n}$ is a complex Gaussian noise vector. In general, the entries of $\mathbf{H}_k$ are governed by random fading processes and in theoretical work these are often modelled as independent (or partially correlated) complex Gaussian variables [8]. This results in a matrix of random variables, $\mathbf{H}_k$ (with the sans-serif typeface denoting a matrix of random variables), of which the rank is $\min(M, N)$.

For MIMO to work there must be at least some degree of multipath propagation that ensures decorrelation between receive antennas. Within this constraint there are two important extreme cases: predominantly line-of-sight (LOS), in which propagation is governed by Rician fading with only a small multipath propagation component, and non-line-of-sight (NLOS), in which propagation is governed by Rayleigh fading and consists entirely of multipath propagation [23]. LOS scenarios usually result in high correlation between spatial streams due to the reduced impact of multipath fading. MIMO DASs can still experience improved performance in LOS environments due to increased SNR [24].

If $\mathbf{H}_k$ can be measured by the system, many different space-time coding schemes can be applied to improve performance. The highest capacity is achieved using a subset of these schemes termed *spatial multiplexing (SM)* coding schemes [25]. The SM scheme that achieves maximum capacity makes use of the singular value decomposition of $\mathbf{H_k}$:

$$\mathbf{H}_k = \mathbf{U}_k \mathbf{\Sigma}_k \mathbf{V}_k^H \tag{4}$$

where $\mathbf{U}_k$ and $\mathbf{V}_k^H$ are unitary $M \times M$ and $N \times N$ matrices respectively, $\mathbf{A}^H$ denotes the Hermitian transpose of $\mathbf{A}$ and $\mathbf{\Sigma}_k$ is a diagonal matrix whose entries are the singular values of $\boldsymbol{H}_k$. By using $\mathbf{V}_k$ as a pre-coding matrix and $\mathbf{V}_k^H$ as a post-coding matrix an equivalent channel can be formed as:

$$\mathbf{y} = \mathbf{U}_k^H \mathbf{H}_k \mathbf{V}_k \mathbf{x} + \mathbf{U}_k^H \mathbf{n} \tag{5}$$

where $\hat{\mathbf{n}} = \mathbf{U}_k^H \mathbf{n}$ is an adjusted noise term. This SM scheme is termed *multiple eigenmode transmission* because the channel is now represented as several orthogonal eigenchannels of the original channel scaled by the singular values of $\mathbf{H}_k$.

The optimal power allocations for each eigenchannel to maximise capacity can be determined using the well-known water filling algorithm [26]. Implementation of a multiple eigenmode transmission scheme is only possible if $\mathbf{H}_k$ as measured at the receiver is fed back to the transmitter periodically, which can incur significant overhead and increase system complexity. As a result, in many practical MIMO systems $\mathbf{H}_k$ is not known at the transmitter. However, by estimating the channel matrix at the receiver using *successive interference cancellation (SIC)*, *zero forcing (ZF)* or *minimum mean square error (MMSE)*, such as in Bell Labs' V-BLAST algorithm, it is possible to approach the capacity of a multiple eigenmode transmission scheme with uniform power allocation across all eigenmodes [27]. Further, at sufficiently high transmit SNR, such as found in many indoor DASs, the uniform power and water filling methods converge [25]. Consequently, the multiple eigenmode transmission channel capacity with uniform power allocation is used in this paper as the channel capacity for all MIMO systems unless stated otherwise. Capacities for water filling power allocation schemes are included for reference.

Using uniform power allocation, the total Shannon capacity of the channel $\boldsymbol{H}_k$ is simply the sum of the Shannon capacities of all the eigenchannels:

$$C_k = B \sum_{p=1}^{S} \log_2 \left(1 + \frac{\rho}{M} \sigma_{k,p}^2\right) \tag{6}$$

where B is the bandwidth of the channel, ρ is the total signal to noise ratio of the system and $\sigma_{k,p}$ is the p^{th} largest magnitude

singular value of $\mathbf{H}_k$.

If perfect Rayleigh fading exists in the channel then $\mathbf{H}_k$ will be unitary and all eigenchannels will have equal capacity. In reality, there is often correlation between the entries of $\mathbf{H}_k$ and so some of the eigenchannels will have lower equivalent SNR. As a result the spatial multiplexing gain is reduced. The spread of singular values (or equivalently eigenvalues), and hence degree of possible spatial multiplexing, can be quantified by the condition number, K, of the channel matrix $\mathbf{H}_k$. This number is often expressed in dB as

$$K_k = 20\log_{10}\left(\frac{\max\limits_{p}(\sigma_{k,p})}{\min\limits_{p}(\sigma_{k,p})}\right) \tag{7}$$

where K_k is the condition number in dB, $\sigma_{k,p}$ represents the p^{th} singular value of the channel matrix $\mathbf{H}_k$, $\max\limits_{p}(\sigma_{k,p})$ represents the maximum $\sigma_{k,p}$ across all p, and $\min\limits_{p}(\sigma_{k,p})$ represents the minimum $\sigma_{k,p}$ across all p.

The level of spatial correlation is intimately linked to the angular distribution of power at the transmitter and receiver – the more uniform (non-directional) this distribution is the lower the spatial correlation and the higher the spatial multiplexing gain [25], [28]. This follows from the scattering nature of multipath fading – radiation arriving at all angles must have been scattered heavily by a rich multipath environment and so will exhibit a highly random distribution. By contrast, in the case where there is strong line-of-sight from the transmitter to the receiver the distribution of power will consist of a large directional and deterministic component and a smaller random component, resulting in higher spatial correlation and a higher condition number.

In the case where multiple RAUs are transmitting the same spatial streams, the $\mathbf{H}_k$ matrices from each RAU are added to get the total channel response, $\mathbf{H}$, which can be used in place of $\mathbf{H}_k$ to find the capacity in equation 6. In a system with ability to feed channel information to the transmitter, it is possible to adjust the phase shift of each spatial stream at each RAU independently in order to minimize the condition number of $\mathbf{H}_k$, a restricted form of transmit beamforming. This allows an examination of the performance under conditions of minimized spatial correlation for an of a $M \times N$ MIMO DAS with replication factor $R > 1$ uniform power allocation across eigenchannels. Just as with water filling, this scheme requires knowledge of the channel to be fed back to the transmitter thereby adding overheads and complexity. However, it is included in this paper for reference.

To provide an indication of the benefit offered by MIMO DAS it is necessary to compare its performance to a DAS using an optimal diversity scheme with no spatial multiplexing. *Maximal ratio combining* (MRC) is one such scheme that provides the maximum possible SNR at the receiver when the signals from each of the receive antennas are added [29]. There are other sub-optimal combining schemes such as equal gain combining and selection combining [25]. The latter, which selects the most powerful signal from all the receive antennas, is often used due to its greater simplicity of implementation. Both MRC and selection combining are examined here to ensure a fair comparison between SM and non-SM schemes.

In order to determine channel capacity, experimental MIMO work either measures realizations of $\mathbf{H}_k$ directly under a range of fading conditions or else extracts parameters of the underlying statistical channel behaviour [30]. In either case, it is desirable to test a range of multipath fading scenarios, or realizations of $\mathbf{H}_k$. This allows a more generalized overview of performance that is less dependent on the nuances of a particular fading environment and reflects higher-level design features such as whether LOS or NLOS propagation is more dominant. Quantities such as Shannon capacity or condition number are then represented by probability distributions that can be compared for different cases. In this paper, the cumulative distribution functions (CDFs) of such quantities are used.

B. Multi-user MIMO

A basic multiuser MIMO system consists of a base station serving multiple users on the downlink, termed the *MIMO broadcast channel*, and multiple users sending data to a single base station on the uplink, termed the *MIMO multiple access channel*. This paper centres on the design of wireless access systems rather than mobile terminals and so only the MIMO broadcast channel is considered. However, the performance of this is intimately related to that of the multiple access channel [31].

It is well known that *dirty paper coding (DPC)* is the optimal method of sharing a MIMO broadcast channel amongst many users [32]. However, such advanced multiuser MIMO techniques are complex to implement and are not yet used in real MIMO services such as 802.11n, although basic implementations are planned for future systems such as 802.11ac. It has also been shown for $M \times N$ where $M/N \approx 1$ that as the SNR increases the performance of DPC offers little improvement over *time division multiple access* (TDMA) [33]. Because the systems examined here have relatively large SNR ($>$ 20dB) and have similar numbers of antennas on the transmit side as on each mobile receiver (e.g. 3×3 MIMO), only TDMA is considered in multi-user capacity analyses.

A TDMA system can be considered to behave as the sum of several single user systems. For a TDMA system with a base station, q, serving P users, the aggregate capacity is a random variable given by:

$$C_{q\ \mathrm{agg}} = \sum_{p=1}^{P} w_p C_p \tag{8}$$

where

$$\sum_{p=1}^{P} w_p = 1 \tag{9}$$

and C_p is a random variable representing the capacity available to the p^{th} user, determined from equation 6, and w_p is the weighting allocated to this user. In the case examined here with equal resource allocation, $w_p = \frac{1}{P}$. The resultant probability density function of $C_{q\ \mathrm{agg}}$ can be computed from the probability density functions for C_1 through C_P using random variable analysis.

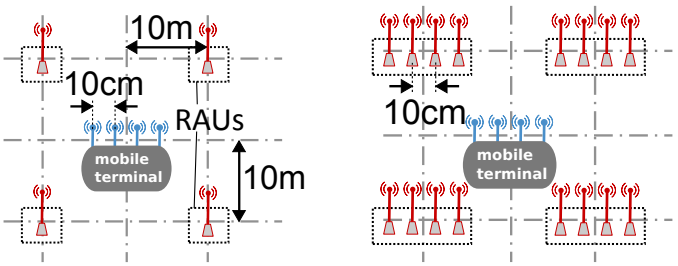

Fig. 2. Layout of two theoretical MIMO DAS scenarios: (a) 4×4 system with replication $R = 1$ and (b) 4×4 system with replication $R = 4$.

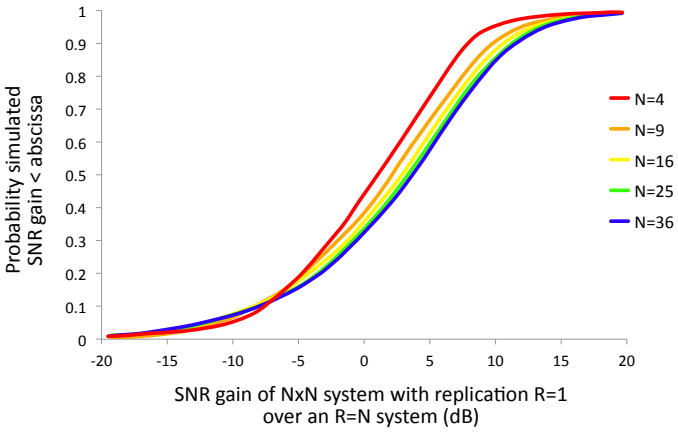

Fig. 3. Graph showing the SNR gain for an $N \times N$ MIMO DAS with replication $R = N$ as N is increased.

If there are Q separate base stations each serving different sets of users due to different spatial locations or different frequency resources, the total aggregate capacity of the network is:

$$C_{\text{agg}} = \sum_{q=1}^{Q} C_{q\ \text{agg}} \tag{10}$$

where C_{agg} is the aggregate capacity for the q^{th} base station as defined in equation 8. Again, the resultant probability density function for C_{agg} can be computed from the probability density functions of $C_{q\ \text{agg}}$ for $q = 1 \ldots Q$.

In a *multichannel DAS*, multiple base stations operate over the same broadband DAS infrastructure using different frequency channels. An example of this is shown in figure 1. When accessed by multiple users is assumed that both time and frequency resources are shared between users with each user adopting the frequency channel of a particular base station and then time sharing with other users on that same channel.

III. Simulated comparison of $N \times N$ DAS layouts

It is first necessary to compare theoretically the performance of $N \times N$ with replication $R = 1$ configurations to $N \times N$ with replication $R = N$ configurations. Full simulation of MIMO systems is difficult because it requires modeling of complex fading environments. Using a simple illustrative example, however, it can be seen that for small numbers of spatial streams the SNR performance of an $N \times N$ with $R = 1$ configuration approaches that of a $N \times N$ with $R = N$ configuration. Consider the two systems shown in figure 2 representing a 4×4 with $R = 1$ and a 4×4 with $R = 1$ MIMO DAS respectively. It is assumed that the average power transferred is the same across all possible pairs of transmit and receive antennas for a particular RAU and mobile terminal. This is because the antenna spacings within each RAU are much less than spacings between RAUs. The effects of fading are not included and instead the propagation loss over a distance is a used as an indicator of the mean statistical SNR.

The 802.11n standard specifies that receivers should be able to detect signals with powers as low as -82dBm over a 20MHz bandwidth channel [34]. Given this, a typical 802.11n receiver would be expected to have a noise floor less than -90dBm over this bandwidth. Transmit power for 802.11n access points is usually 10-20dBm and so in a typical scenario there might be a transmit power of 15dBm per RAU, with this power being uniformly distributed between the multiple transmit antennas. These test values are then used here and throughout rest of this paper.

The spacing between antennas at each RAU and on the mobile terminal is 10cm, corresponding to about 0.8 wavelengths at 2.4GHz. This spacing creates sufficient antenna decorrelation in fading environments for MIMO to operate effectively. It is assumed for this simulation that the 3dB bandwidth of each antenna is much greater than 100MHz, enough to support any 802.11n channel in the 2.4GHz band.

The SNRs at all receive antennas for both the 4×4 MIMO DAS with $R = 1$ and 4×4 MIMO DAS with $R = 4$ cases are calculated at every point on a grid of 0.5m spacings. The free-space propagation loss used for this is calculated using the Friis transmission equation. Next, the ratio of the SNRs for the $R = 4$ MIMO DAS and the $R = 1$ MIMO DAS, termed the *SNR gain*, is calculated at each location. The SNR gains at every receive antenna at every point in the room are collated to produce a CDF. This CDF shows the proportion of points in the room that experience an SNR gain from the 4×4 with the $R = 4$ configuration.

This process is repeated for larger systems (9×9, 16×16 etc). The spacing between RAUs is kept constant to simulate realistic DAS installations in which it is impractical and expensive to place RAUs too closely. The transmit power per RAU is kept constant as N is increased to ensure a fair comparison. The resultant CDFs are plotted in figure 3. It is seen that the SNR gain of $N \times N$ MIMO DASs with $R = N$ over $N \times N$ MIMO DASs with $R = 1$ increases with N. For example the median SNR gain increases from 0.9dB in the 4×4 MIMO DAS configuration to 2.2dB in the 9×9 MIMO DAS configuration. As N decreases, the median SNR gain tends towards 0dB indicating that there is minimal overall SNR improvement of $N \times N$ MIMO DAS with $R = N$ over $N \times N$ MIMO DAS with $R = 1$ for small N.

The reason for this increase in SNR gain can be understood by considering the distance from each antenna on the mobile terminal to the nearest transmitting antenna for each spatial stream. For the $R = N$ case this distance is the same for

every spatial stream because every RAU transmits every spatial stream. In the $R = 1$ case, however, some spatial streams are much further away from the mobile terminal than others. Because the distance between RAUs is kept constant, in this configuration the distance of the furthest spatial streams from the mobile terminal increases with N. This results in increased propagation loss of these spatial streams lowering their SNR. For small N this SNR reduction is counteracted by the greater transmit power per spatial stream at each RAU in the $R = 1$ configuration. This is why the two configurations offer similar performance for small N.

In MIMO systems with relatively high receive SNR (>20dB) increases in channel capacity are strongly linked to SNR and are less affected by changes in spatial correlation properties of the channel [18]. This link is particularly strong in environments with high spatial correlation, for example due to significant line-of-sight propagation as in this case [35]. Since for small values of N (2,3 or 4) the $N \times N$ MIMO DAS with $R = N$ and $N \times N$ MIMO DAS with $R = 1$ configurations exhibit similar SNR properties, it can then be said that they will have similar channel capacities. However, in future MIMO systems that have many more spatial streams, such as 802.11ac, this similarity no longer holds and it may be necessary to use $N \times N$ MIMO DAS with $R = N$ configurations to fully exploit the capacity gains of MIMO transmission.

It should be noted that systems with larger N have the added disadvantage that they require N separate RF chains comprising mixers and analog-to-digital converters. Their complexity, cost and energy usage thus scales linearly with N [36]. Moreover, systems with $R = N$ require N separate RF amplifiers at each RAU, meaning they require on average N times as many amplifiers as $R = 1$ systems. Because an increase in N from 4 to 9 (i.e. 3.5dB) only offers a 1.3dB increase in SNR gain, a sub-linear improvement, there are diminishing returns in terms of SNR of the $R = N$ configuration as N is increased.

IV. Experimental set-up

Figure 4a shows the experimental system used to measure the 3×3 MIMO channel. A vector network analyzer (VNA) is used to take measurements at 1600 channels over a frequency range of 1.7GHz to 2.7GHz. This range is sufficient to create many different multipath interference scenarios and is limited due to the frequency response of the antennas.

Careful measurements of the frequency responses of the RoF links and the antennas in isolation are taken. The antennas used are dipoles that are omnidirectional in the azimuth plane and are measured to have a 3dB bandwidth of 390MHz centred at 2.497GHz. Over the 1GHz frequency range used for these experiments the gain of the antennas varies by 25dB due to reduced efficiency but because the VNA uses a narrowband filter when taking measurements, the noise at the receiver is sufficiently low that even with such high attenuation the received SNR is >30dB. This means that the channel coefficients can still be measured accurately with these antennas and can be equalized using the antenna response measurements taken in isolation.

The antenna and RoF link response measurements are used along with the Friis transmission equation to calibrate the measurements so as to remove frequency effects and ensure that only the broadband propagation channel is measured. Each calibrated measurement can then be considered to represent a different frequency-independent fading scenario [37]. The average gain of the combined transmit and receive antennas and RoF link is measured as -12dB and this is incorporated into the calibrated channel measurements to represent realistic performance. A PC driving an ARM microcontroller switches the transmit and receive arrays via two RF switches to allow measurement of one channel coefficient at a time. As discussed in section III, a typical 802.11n system operates on a 20MHz bandwidth channel with a transmit power of 15dBm and a receiver noise floor of -90dBm [34]. These values, normalized to a 1Hz bandwidth, are used here for channel capacity calculations.

Such measurements can be corroborated by measuring *throughput*, which provides an indication of the actual data rates achievable using existing technology, for example 802.11n. The throughput of the channel is tested using the setup shown in figure 4b with parameters as listed in table I. The access point used is a TrendNET 690AP 802.11n capable of utilizing up to 3 independent spatial streams. The receiver is a laptop with an Intel Centrino 6300 Ultimate-N wireless card installed, also capable of utilizing up to 3 spatial streams. Throughput testing is done with the *Iperf* package. UDP packets are sent down the link at 100 Mbps and the packet loss rate is used to determine the achievable throughput of the link.

The IEEE 802.11n standard defines 77 different possible *modulation and coding schemes (MCS)* that can be used to adjust the data rate on each spatial channel. For example, MCS 0 represents a single spatial stream using BPSK at a coding rate of $1/2$ [34]. In a realistic situation the MCS would be allowed to change dynamically to adjust to the channel conditions. However for the throughput experiment presented here the access point is forced to use MCS 17 so that 3 equal-rate spatial streams are always being used, thereby exclusively testing 3×3 MIMO functionality. To enable comparison of throughput performance with a fixed-rate MCS, UDP traffic is sent down the link at a much greater rate than the channel can support. The receiver can then determine the proportion of packets that were received error-free to give an indication of the maximum achievable data rate of the link. UDP is used to avoid the additional retransmission overhead and delays inherent to TCP.

The DAS used in both cases is a Zinwave 2700, which provides 30m RoF links over OM1 MMF.

Measurements are taken for a range of different DAS configurations in two typical indoor DAS scenarios as shown in figure 5. One of the test environments has a significant LOS between each RAU and the receiver while the other is entirely reliant on NLOS propagation. Because the room used contains many items, such as metal equipment racks and tables, there is sufficient multipath fading that spatial multiplexing can be achieved even for the LOS case as discussed in section I. These then represent two quite different

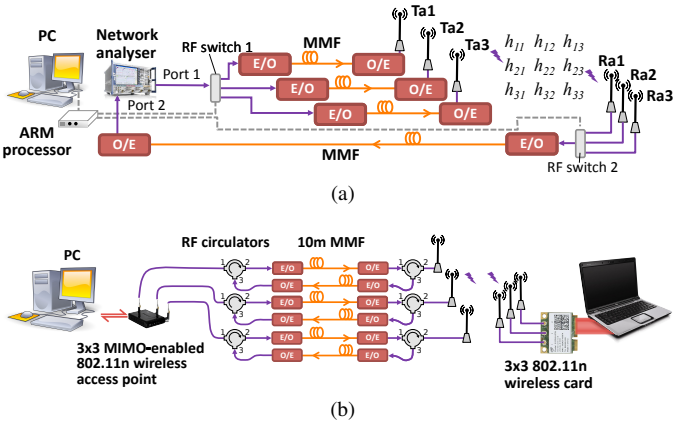

Fig. 4. Experimental set-up of: (a) 3×3 MIMO channel measurement system and (b) 3×3 MIMO 802.11n throughput testing system.

TABLE I
PARAMETERS OF THROUGHPUT TESTING SETUP

Parameter		Value
Frequency		2.4 GHz
MCS index	17	QPSK, coding rate 1/2
		3 spatial streams
		Max data rate: 43.3 Mbps
Channel bandwidth		20 MHz
A/P Transmit power		15 dBm
RoF link gain		-30 dB

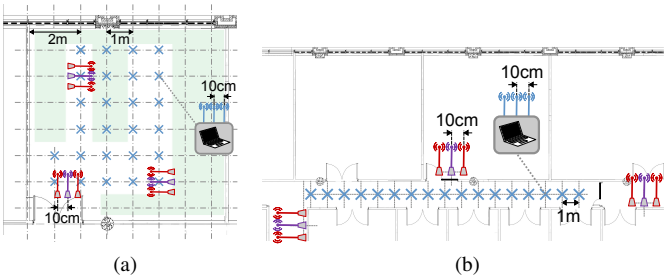

Fig. 5. Test propagation environments showing location of transmit antennas and receiver test points: (a) line-of-sight scenario (b) non line-of-sight scenario.

but realistic scenarios. Measurements are taken at multiple points in both environments to evaluate the performance over a coverage area. In both cases the transmit and receive antennas at each RAU are spaced 10cm apart. The 3×3 with $R = 3$ configuration is tested by measuring the 3×3 CAS response 3 times with the transmit antennas at different RAU locations each time. It is ensured that room is kept static between these measurements. The 3×3 with $R = 1$ configuration is tested by using the center antenna of each group of 3 transmit antennas tested in the 3×3 MIMO DAS with $R = 3$ configuration.

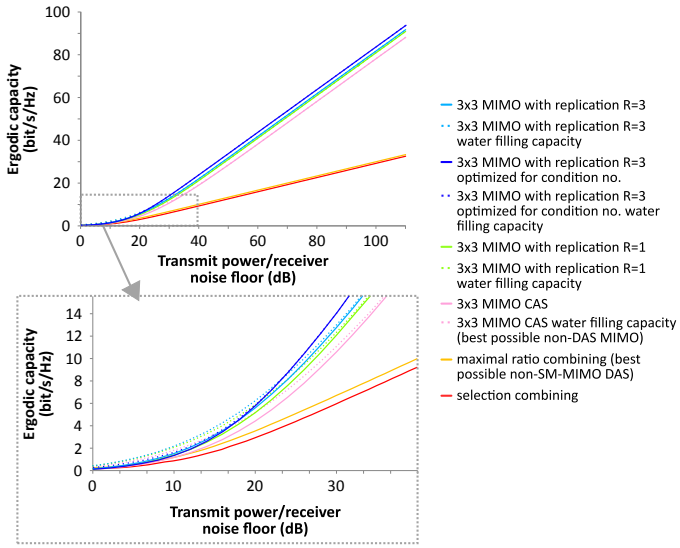

Fig. 6. Ergodic channel capacity as a function of transmit power relative to the receiver noise floor taken across all fading scenarios and measurement locations in the LOS propagation scenario.

V. SINGLE USER RESULTS

A. Capacity

Figure 6 shows the ergodic channel capacity for the LOS propagation scenario as transmit power is increased relative to the receiver noise floor. It can be seen that once the transmit power is about 20dB above the receiver noise floor, the capacity becomes strongly linearly dependent on SNR in agreement with previous findings as discussed in section I. This is further evident from the fact that the waterfilling power allocation and uniform power allocation schemes begin to converge after this point. This region with high (>20dB) margin between transmit power and receiver noise floor is where many indoor wireless systems operate and so is of particular interest.

The advantage of MIMO over diversity schemes such as maximal ratio combining and selection combining is clear from figure 6. However, of greatest interest to the design of MIMO-enabled DAS is the difference between alternative DAS layout schemes. First, it is seen that all MIMO DAS schemes outperform MIMO CAS in terms of capacity by at least 3.1 bit/s/Hz in the region of interest. The optimal capacity is achieved with the 3×3 with $R = 3$ MIMO DAS with the phase at each RAU adjusted (i.e. beam-forming) to optimize condition number. However, just as with waterfilling this requires channel knowledge at the transmitter so is expensive and less efficient to implement, not to mention incompatible with commonly used algorithms such as V-BLAST. The most significant observation is there is very little improvement of the 3×3 MIMO DAS with $R = 3$ layout over the 3×3 MIMO DAS with $R = 1$ layout, the former offering only a 1.0 bit/s/Hz advantage in the region of interest. When the transmit power is 20dB above the receiver noise floor, i.e. a 20dB *transmit power margin*, the $R = 3$ scheme offers an 8% capacity increase. However, for a more typical transmit power margin of 90-120dB this improvement reduces to 1%.

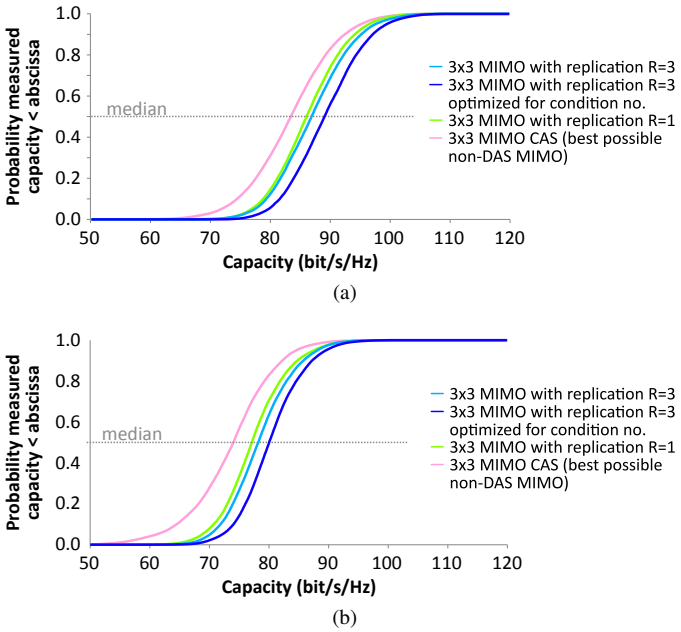

Fig. 7. CDF of aggregate network capacity for a single user for two propagation scenarios: (a) LOS case and (b) NLOS case

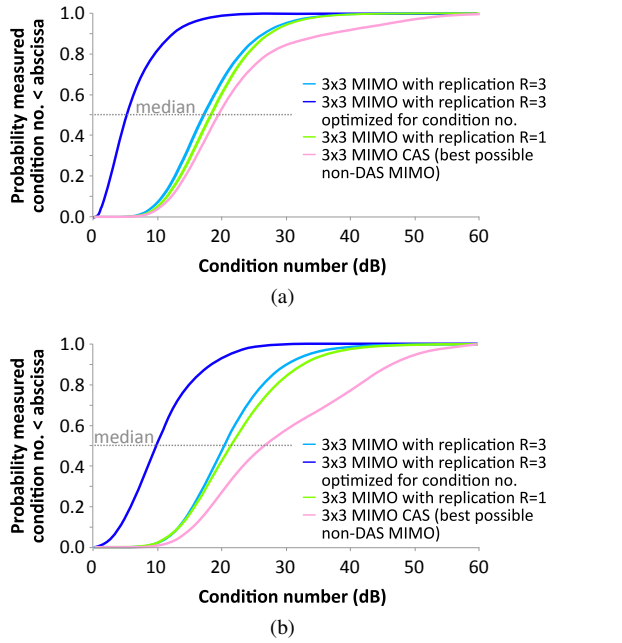

Fig. 8. CDF of condition number for a single user with in two scenarios: (a) LOS case and (b) NLOS case

Next, the statistical fading behaviour is examined for a fixed transmit power of 15dBm and receiver noise floor of -90dBm. The measured CDF of channel capacities for the LOS and NLOS scenarios, showing the difference between the 3×3 with $R = 3$ and 3×3 with $R = 1$ DAS configurations are presented in figure 7a and figure 7b respectively. The CDFs are taken over all measured multipath fading scenarios and at all measurement locations so that they represent the probability of achieving a certain channel capacity over all possible fading environments and locations. Again, the improvement of MIMO DAS over MIMO CAS and diversity schemes is evident. As before a scheme using beam-forming to minimize condition number is included as a reference because it represents the capacity achievable for a 3×3 with $R = 3$ system if channel knowledge were fed back to the transmitter.

It can be seen that for the LOS case in figure 7a the MIMO DAS offers a significant performance improvement over MIMO CAS or diversity schemes. Further, the 3×3 with $R = 1$ MIMO DAS offers capacity comparable to the 3×3 with $R = 3$ MIMO DAS. The 3×3 with $R = 1$ median capacity of 86.2 bit/s/Hz is just 0.8% short of the capacity offered by a 3×3 with $R = 3$ MIMO DAS. This compares to the 3.2% capacity shortfall when using a MIMO CAS.

The same is true of the NLOS case shown in figure 7b and it is seen that the median capacity of the 3×3 with $R = 1$ MIMO DAS is 77 bit/s/Hz, 1.4% short of the 3×3 with $R = 3$ case. This compares to the 4.1% capacity shortfall when using a MIMO CAS in the NLOS case.

Further insight is gained from observing the condition number for the LOS and NLOS cases as shown in figure 8. It is seen for both the LOS and NLOS cases that the condition number for the 3×3 MIMO DAS with $R = 3$ is only marginally better than the condition number for the 3×3 MIMO DAS with $R = 3$ (1.2dB and 1.3dB less respectively). This suggests that there is only a fairly small change in multiplexing gain between the two configurations.

However, there is a more significant improvement in condition number between the MIMO DAS configuration and the MIMO CAS, indicating that the former enables improved spatial multiplexing. This difference is particularly pronounced for the NLOS case. This is to be expected because the strong line-of-sight propagation component creates an uneven angular spread of power at the receiver resulting in high spatial correlation as discussed in section II-A. This should not change, regardless of the location of the transmit antennas. For the NLOS case though the only propagation method is multipath propagation, ensuring a more uniform angular spread of power at the receive antennas. When the antennas are distributed it can be seen from figure 8 that the median condition number reduces by 5.4dB for the NLOS case suggesting that this act further improves the uniformity of the angular spread of received powers. This compares to the LOS case in which the median condition number reduces by only 1.5dB when the antennas are distributed.

These results first show that in both LOS and NLOS cases, 3×3 MIMO DAS with $R = 1$ offers improved capacity over CAS and diversity-only DAS. In predominantly LOS environments the gain is largely due to increased SNR as the condition number is not significantly affected. However in predominantly NLOS cases, both an SNR and condition number improvement are obtained allowing a higher degree of spatial multiplexing.

Furthermore, they show that 3×3 MIMO DAS with $R = 3$ offers only minimal capacity improvement over 3×3 MIMO DAS with $R = 1$, typically of the order of 1%. This is a particularly relevant fact as the former designs have the significant disadvantage of requiring additional cabling or broadband multiplexing schemes to operate when compared

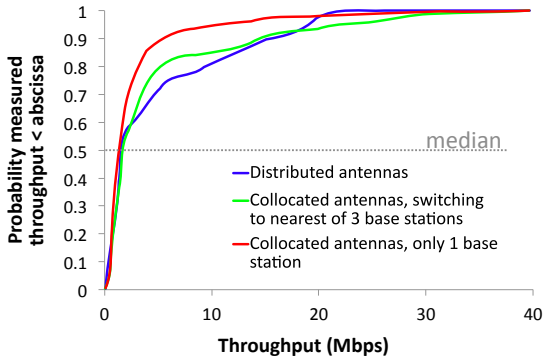

Fig. 9. CDF showing improvement in throughput of using MIMO DAS with 3×3 802.11n compared with CAS

with the latter, which can be implemented using pre-existing DAS installations. On balance then, it seems that the 3×3 MIMO DAS with $R = 1$ offers a lower-cost solution with comparable performance.

B. Throughput

Previous throughput measurements have shown MIMO DAS to offer an improvement over MIMO CAS for a 2×2 MIMO system [38]. However, throughput for a 3×3 MIMO DAS configuration has not been investigated nor has it been compared with the case of having additional base stations in place of a DAS.

Figure 9 shows the measured throughput for a 3×3 MIMO DAS with $R = 1$ compared with MIMO CAS in the LOS scenario, for both a single base station and the case with separate 3×3 MIMO CAS base stations in place of each RAU. For low values of throughput, there is shown to be little difference in the CDF curves. However, at higher throughputs it is seen that the MIMO DAS offers improved performance over the CAS case. A smaller improvement over the case with separate base stations is also observed. This suggests that under realistic MIMO test conditions, a 3×3 MIMO DAS with $R = 1$ offers improved throughput performance over a CAS. This is consistent with the results for Shannon capacity presented in section V-A.

VI. Multiple User Results

A. Single base station

The capacity of a DAS where there are multiple users served by a single base station is now examined. Figure 10 shows the total aggregate capacity of a system as the number of users is increased for two cases: the first with a single base station and the second 3 base stations. This is done for two different system configurations – a CAS with separately located base stations and a DAS with collocated base stations operating on separate frequency channels, an example of which was shown in figure 1. The results are shown in shown in figure 10a and figure 10b respectively.

It can be seen that in both cases if only a single base station is used there is an upper limit on the aggregate capacity as the number of users is increased. This upper limit shifts

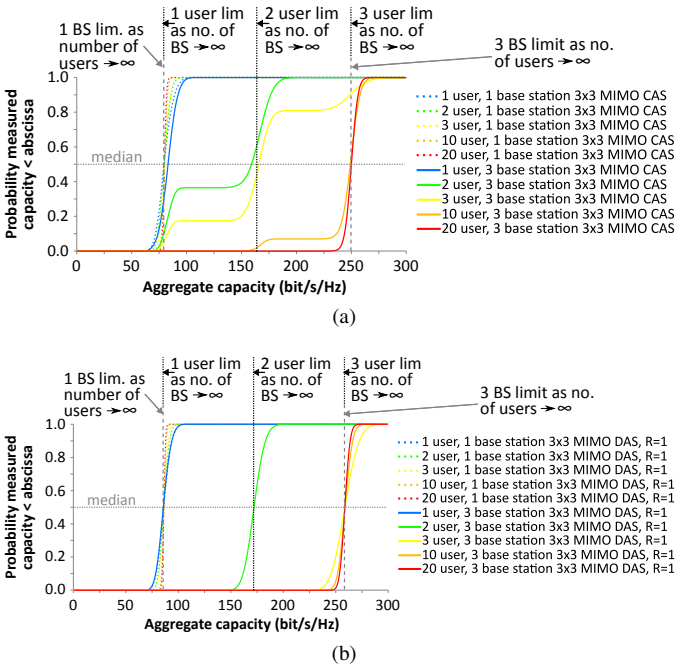

Fig. 10. CDF of aggregate network capacity comparing capacity for a single base station with multiple base stations in the LOS scenario for two cases: (a) collocated antenna system and (b) distributed antenna system.

significantly higher when additional base stations are added. In fact, this upper limit is simply N times the median capacity for a single base station, provided that the number of users is $\gg N$. This indicates that additional base stations are a necessary requirement for adding capacity to a system.

If the number of base stations is increased for a fixed number of users the capacity will also approach a limit, as shown in figure 10. In fact, it is seen that the two-user limit coincides with observed step-like changes in the CDF. This is because the two-user limit represents the capacity limit when two users are being served by separate base stations. In CAS scenarios, there is a possibility that even if only two users are present, they will be located in such a way that they are both served by the same base station even if there are other unused base stations. This results in regions of reduced aggregate capacity, indicated by the step-like behaviour observed in figure 10a. These steps are not observed in figure 10b because capacity can always be shared between base stations when they are centrally located as in a multichannel DAS.

B. Multiple base stations

Finally, it is necessary to examine the scenario where multiple users are served by multiple base stations. This is the scenario of greatest practical importance for future wireless systems. This is achieved in a CAS by installing additional base stations at new locations or in a DAS by connecting additional base stations to the same DAS infrastructure and operating them on unique non-overlapping frequency channels, as is possible in 802.11a, 802.11g and 802.11n systems. The 802.11n standard defines 3 non-overlapping 20MHz channels in the 2.4GHz band and 21-27 non-overlapping 20MHz channels in the 5GHz band (depending on local regulations),

so there is much scope for implementing such a system. The downside of this approach is that it reduces frequencies available to neighbouring DAS installations and creates greater potential for interference. Each user still uses a 20MHz bandwidth channel and may only connect to a base station operating on that same channel. Users accessing the same base station share time slots, as discussed in section II-B.

The aggregate capacity for multiple users accessing multiple base stations is shown in figures 11a and 11b for the LOS and NLOS cases respectively. A multichannel DAS running several base stations simultaneously is compared to the case of installing separate CAS MIMO base stations at each of the DAS RAU positions.

It is seen that both configurations are able to significantly increase aggregate capacity. However, the multichannel DAS provides more uniform coverage than the separate CAS base station configuration as indicated by the presence of step-like behaviour in the CAS curves in figure 11. As discussed in section VI-A this step-like behaviour arises because in a CAS, performance is more dependent on the distribution of users in the coverage area. For example, a multichannel DAS would cope just as well if all users were located very close to one RAU whereas in a CAS the capacity would be limited to the multiple-user single base station case.

As discussed in section VI-A, when the number of users is much larger than the number of base stations an upper limit on the aggregate capacity is approached. In the LOS scenario, this limit is 259 bit/s/Hz for the 3×3 MIMO DAS with $R=1$ case, 0.8% less than the limit for the 3×3 MIMO DAS with $R=3$ case at 261 bit/s/Hz. Similarly for the NLOS scenario this limit is 233 bit/s/Hz for the 3×3 MIMO DAS with $R=1$ case, 1.3% less than the limit for the 3×3 MIMO DAS with $R=3$ case at 236 bit/s/Hz. The separate base station CAS configuration provides the lowest of the upper capacity limits with 250 bit/s/Hz and 217 bit/s/Hz for the LOS and NLOS scenarios respectively.

It can also be seen that a 3×3 MIMO DAS with $R=1$ multichannel DAS can offer multi-user median aggregate capacities 3.4% and 7.3% greater than having separate MIMO CAS base stations for LOS and NLOS scenarios respectively. Clearly, DAS has an important role to play in delivering capacity for multi-user multiple base stations scenarios. Further, 3×3 MIMO DAS with $R=1$ multichannel DAS are sufficient to offer this additional support as they offer comparable median aggregate capacity to 3×3 MIMO DAS with $R=3$ multichannel DAS.

It should be noted that the different configurations each have their own drawbacks. Multichannel DAS can create problems with inter-cell interference as they use many frequency channels over the same spatial region. For advanced DAS features, such as dynamic capacity allocation, additional hardware is needed to be able to sense and process the user environment, increasing system cost. 3×3 MIMO DAS with $R=3$ have the disadvantage of requiring additional multiplexing infrastructure or additional fibres to transport multiple MIMO streams to single RAUs. Because 3×3 MIMO DAS with $R=1$ can be deployed using pre-existing non-MIMO DAS infrastructure this makes them a cheaper option than 3×3 multichannel DAS with $R=3$. However, as discussed in section III the difference in capacities between the two designs may increase with higher numbers of spatial streams making $N\times M$ DAS with $R=N$ a more attractive option if high capacity is required.

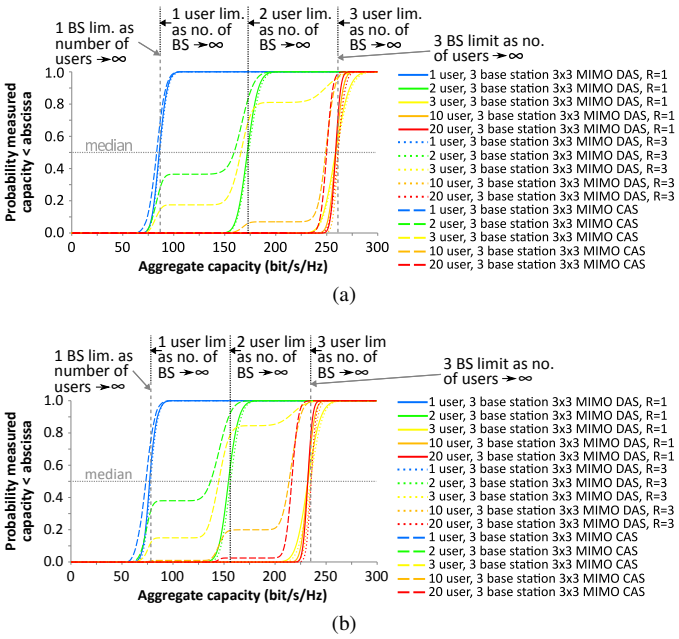

Fig. 11. CDF of aggregate network capacity for multiple users with multiple base stations for two scenarios: (a) LOS and (b) NLOS.

VII. Conclusion

This paper compares different design configurations of MIMO DAS and examines their effect on capacity and throughput performance. First, it is shown theoretically that in terms of SNR, $N\times N$ MIMO DAS with antenna replication $R=N$ only offers improvement over $N\times N$ MIMO DAS with antenna replication $R=1$ for larger values of N (≥ 4).

Next, it is confirmed experimentally that a 3×3 MIMO DAS offers improvement in capacity and throughput compared with a MIMO CAS for a 3×3 system in two typical indoor DAS scenarios offering 3.2% and 4.1% improvement in capacity respectively. It is then shown for both single both single user and multiple user scenarios using single and multiple base stations that a 3×3 MIMO DAS with antenna replication $R=1$ can achieve similar performance to a 3×3 MIMO DAS with antenna replication $R=3$. For the multichannel 3×3 MIMO DAS with antenna replication $R=1$ and 20 users, median aggregate capacities of 259 bit/s/Hz and 233 bit/s/Hz are achieved for the two typical propagation scenarios respectively. These are only 0.9% and 1.4% short of the aggregate capacities for the multichannel 3×3 MIMO DAS with antenna replication $R=3$ respectively.

It is concluded that existing DAS infrastructure can be used to deploy 3×3 MIMO-enabled DAS with antenna replication $R=3$ incurring minimal capacity penalty and without the need for additional fibers or multiplexing schemes.

To meet the demands of tomorrow's communication networks with high densities of users demanding high data rates

it will be necessary to install more base stations per unit area to enable increased aggregate capacity. These results show that DAS has an important role to play because it is able to further improve on the performance of separately located base stations while offering additional flexibility.

ACKNOWLEDGEMENT

The authors would like to thank Kun Zhu, Adrian Wonfor, the U.K. Engineering and Physical Sciences Research Council (EPSRC) and the Rutherford Foundation of the Royal Society of New Zealand for their support.

REFERENCES

[1] "Key Global Telecom Indicators for the World Telecommunication Service Sector," ITU, Tech. Rep., 2011.

[2] "Cisco Visual Networking Index : Global Mobile Data Traffic Forecast Update , 2011 2016," Cisco Systems, Tech. Rep., 2012.

[3] "Visible light communication (vlc) - a potential solution to the global wireless spectrum shortage," GBI Research, Tech. Rep., 2011.

[4] T. Norman, "Research forecast report - Wireless network traffic 2010-2015: forecasts and analysis," Analysys Mason, Tech. Rep., 2010.

[5] P. Chow, A. Karim, V. Fung, and C. Dietrich, "Performance advantages of distributed antennas in indoor wireless communication systems," *Proc. 1994 IEEE Vehicular Technology Conference*, Stockholm, Sweden, 1994.

[6] M. J. Crisp, S. Li, A. Wonfor, R. V. Penty, and I. H. White, "Demonstration of a Radio over Fibre Distributed Antenna Network for Combined In-building WLAN and 3G Coverage," in *Proc. 2007 Optical Fiber Communication and the National Fiber Optic Engineers Conference*, Anaheim, USA, Mar. 2007.

[7] "Femtocells and Distributed Antenna Systems Complementary or Competitive?" ABI Research, Tech. Rep., 2009.

[8] D. Gesbert, M. Shafi, P. Smith, and A. Naguib, "From theory to practice: an overview of MIMO space-time coded wireless systems," *IEEE J. Sel. Areas Commun*, vol. 21, no. 3, pp. 281–302, Apr. 2003.

[9] R. Stacey *et al.*, "IEEE 802.11-09/0992r21 - IEEE P802.11 Wireless LANs Specification Framework for TGac," 2011. [Online]. Available: https://mentor.ieee.org/802.11/dcn/09/11-09-0992-21-00ac-proposed-specification-framework-for-tgac.doc.

[10] M. Alatossava *et al.*, "Measurement Based Capacity of Distributed MIMO Antenna System in Urban Microcellular Environment at 5.25 GHz," in *Proc. 2008 IEEE Vehicular Technology Conference Spring*, Singapore, May 2008.

[11] K. Miyamoto *et al.*, "Experimental demonstration of MIMO RF signal transmission in RoF-DAS over WDM-PON," *Proc. 2011 International Topical Meeting on Microwave Photonics*, Singapore, Oct. 2011.

[12] A. Chowdhury *et al.*, "Multi-service Multi-carrier Broadband MIMO Distributed Antenna Systems for In-building Optical Wireless Access," in *Proc. 2010 Optical Fiber Communication and National Fiber Optic Engineers Conference*, San Diego, 2010.

[13] G. Gordon, J. Carpenter, M. Crisp, T. Wilkinson, R. Penty, and I. White, "Demonstration of Radio-over-Fibre Transmission of Broadband MIMO over Multimode Fibre using Mode Division Multiplexing," in *Proc. 2012 European Conference and Exhibition on Optical Communication*, Amsterdam, 2012.

[14] K. Zhu, M. J. Crisp, S. He, R. V. Penty, and I. H. White, "MIMO System Capacity Improvements Using Radio-over- Fibre Distributed Antenna System Technology," in *Proc. Optical Fiber Communication Conference*, Los Angeles, 2011.

[15] R. Ibernon-Fernandez, J.-M. Molina-Garcia-Pardo, and L. Juan-Llacer, "Comparison Between Measurements and Simulations of Conventional and Distributed MIMO System," *IEEE Antennas Wireless Propag. Lett.*, vol. 7, pp. 546–549, 2008.

[16] L. Tarlazzi *et al.*, "Characterization of an Interleaved F-DAS MIMO indoor propagation channel," in *Proc. Loughborough Antennas & Propagation Conference*, Loughborough, UK, Nov. 2010.

[17] W. Roh and A. Paulraj, "MIMO channel capacity for the distributed antenna," in *Proc. IEEE 56th Vehicular Technology Conference*, Vancouver, 2002.

[18] E. Ohlmer *et al.*, "Urban Outdoor MIMO Experiments with Realistic Handset and Base Station Antennas," in *Proc. IEEE 71st Vehicular Technology Conference*, Taipei, 2010.

[19] E. M. Vitucci, L. Tarlazzi, P. Faccin, and V. Degli-Esposti, "Analysis of the performance of LTE systems in an Interleaved F-DAS MIMO indoor environment," in *Proc. 5th European Conference on Antennas and Propagation (EUCAP)*, Rome, Apr. 2011.

[20] D. Gesbert, M. Kountouris, R. Heath Jr., C.-b. Chae, and T. Salzer, "Shifting the MIMO Paradigm," *IEEE Signal Process. Mag.*, vol. 24, no. 5, pp. 36–46, Sep. 2007.

[21] R. W. Heath Jr., T. Wu, Y. H. Kwon, and A. C. K. Soong, "Multiuser MIMO in Distributed Antenna Systems With Out-of-Cell Interference," *IEEE Trans. Signal Process.*, vol. 59, no. 10, pp. 4885–4899, Oct. 2011.

[22] W. Feng, Y. Li, J. Gan, S. Zhou, J. Wang, and M. Xia, "On the Deployment of Antenna Elements in Generalized Multi-User Distributed Antenna Systems," *Mobile Networks and Applications*, vol. 16, no. 1, pp. 35–45, Oct. 2009.

[23] P. Kafle, A. Intarapanich, A. Sesay, J. Mcrory, and R. Davies, "Spatial correlation and capacity measurements for wideband MIMO channels in indoor office environment," *IEEE Trans. Wireless Commun.*, vol. 7, no. 5, pp. 1560–1571, May 2008.

[24] S. Büyükçorak and G. K. Kurt, "Spatial Correlation and MIMO Capacity at 2.4 GHz," *Procedia Technology*, vol. 3, pp. 9–17, Jan. 2012.

[25] C. Oestges and B. Clerckx, *MIMO wireless communications : from real-world propagation to space-time code design*, 1st ed. Amsterdam: Elsevier, 2007.

[26] E. Telatar, "Capacity of Multi-antenna Gaussian Channels," *European Transactions on Telecommunications*, vol. 10, no. 6, pp. 585–595, Nov. 1999.

[27] G. Golden *et al.*, "Detection algorithm and initial laboratory results using V-BLAST space-time communication architecture," *Electronics Letters*, vol. 35, no. 1, p. 14, 1999.

[28] G. Foschini, M. Gans, and J. Kahn, "Fading correlation and its effect on the capacity of multielement antenna systems," *IEEE Trans. Commun.*, vol. 48, no. 3, pp. 502–513, Mar. 2000.

[29] T. Lo, "Maximum ratio transmission," *IEEE Trans. Commun.*, vol. 47, no. 10, pp. 1458–1461, 1999.

[30] H. Ozcelik, N. Czink, and E. Bonek, "What Makes a Good MIMO Channel Model?" *Proc. IEEE 61st Vehicular Technology Conference*, Stockholm, Swededen, 2005.

[31] A. Goldsmith, S. Jafar, N. Jindal, and S. Vishwanath, "Capacity limits of MIMO channels," *IEEE J. Sel. Areas Commun.*, vol. 21, no. 5, pp. 684–702, Jun. 2003.

[32] G. Caire and S. Shamai, "On the achievable throughput of a multiantenna Gaussian broadcast channel," *IEEE Trans. Inf. Theory*, vol. 49, no. 7, pp. 1691–1706, Jul. 2003.

[33] N. Jindal and A. Goldsmith, "Dirty-Paper Coding Versus TDMA for MIMO Broadcast Channels," *IEEE Trans. Inf. Theory*, vol. 51, no. 5, pp. 1783–1794, May 2005.

[34] "IEEE Standard for Information technology Telecommunications and information exchange between systems Local and metropolitan area networks Specific requirements Part 11: Wireless LAN Medium Access Control (MAC) and Physical Layer (PHY) Specifications Am," 2009.

[35] C. Eugene, K. Sakaguchi, and K. Araki, "Experimental and analytical investigation of MIMO channel capacity in an indoor line-of-sight (LOS) environment," in *Proc. IEEE 15th International Symposium on Personal, Indoor and Mobile Radio Communications*, Barcelona, Spain, 2004.

[36] A.F. Molisch *et al.*, "Reduced-complexity transmit/receive-diversity systems," in *Proc. IEEE VTS 53rd Vehicular Technology Conference*, Rhodes, Greece, 2001.

[37] A. Saleh and R. Valenzuela, "A Statistical Model for Indoor Multipath Propagation," *IEEE J. Sel. Areas Commun.*, vol. 5, no. 2, pp. 128–137, Feb. 1987.

[38] T. Yamakami, T. Higashino, K. Tsukamoto, and S. Komaki, "An experimental investigation of applying MIMO to RoF ubiquitous antenna system," *2008 International Topical Meeting on Microwave Photonics*, Gold Coast, Australia, September 2008.

Author biographies not included by author request due to space constraints.